Journal of Alloys and Compounds 509 (2011) 535–541

Contents lists available at ScienceDirect

Journal of Alloys and Compounds

journal homepage: www.elsevier.com/locate/jallcom

Promotion of Pt–Ru/C catalysts driven by heat treated induced surface segregation for methanol oxidation reaction

Yu-Chen Wei, Chen-Wei Liu, Wei-Jung Chang, Kuan-Wen Wang*

Institute of Materials Science and Engineering, National Central University, Taoyuan 32001, Taiwan

ARTICLE INFO

Article history:
Received 9 June 2010
Received in revised form
16 September 2010
Accepted 18 September 2010
Available online 25 September 2010

Keywords:
Pt–Ru/C catalysts
Heat treatment
Methanol oxidation
Surface segregation
Degree of alloying

ABSTRACT

Carbon supported Pt–Ru/C (1:1) alloy catalysts supplied by E-TEK are widely used for fuel cell research. Heat treatments in various atmospheres are conducted for the promotion of the methanol oxidation reaction (MOR) and the investigation of the structure–activity relationship (SAR) of the catalysts. The alloy structures, surface compositions, surface species, and electro-catalytic activities of the alloy catalysts are characterized by X-ray diffraction (XRD), temperature-programmed reduction (TPR), X-ray photoelectron spectroscopy (XPS), and cyclic voltammetry (CV), respectively. The as-received Pt–Ru/C catalysts have a Ru rich in the inner core and Pt rich on the outer shell structure. Thermal treatments on the catalysts induce Ru surface segregation in different extents and thereby lead to their alteration of the alloying degrees. O_2 treatment results in obvious Ru segregation and formation of RuO_2. Catalysts treated in H_2 have the highest I_f/I_b value in the CV scans among all samples, indicating the catalysts have the excellent CO de-poisoning ability as evidenced by anodic CO stripping experiments. N_2 treatment may serve as an adjustment process for the surface composition and structure of the catalysts, which can suppress the surface Pt depletion (~60% Pt on the surface), make the components stable and hence promote the MOR significantly.

1. Introduction

The development of the direct methanol fuel cells (DMFCs) and modification of the electrocatalysts has attracted much attention [1–5]. Pt–Ru catalysts are well known to exhibit a superior activity in methanol oxidation reaction (MOR) as discovered more than 30 years ago independently by Watanabe and Petrii [6,7]. A number of review papers summarize the development of Pt–Ru systems [1,7–10]. Up to the present, the Pt–Ru/C anode catalysts of DMFCs still have some shortcomings and need to be improved, such as slow kinetics of MOR and poor CO de-poisoning ability. Many methods, such as addition of modifiers or the third elements, adjustment of preparation parameters, use of alterative supports, and heat treatments on the Pt–Ru catalysts, have been proposed comprehensively in the literature for promotion of home-made catalysts [11–18]. However, the structure–activity relationship (SAR) and promotional effect depends on the preparation methods, alloy structures, and surface compositions of the catalysts significantly, and only some conclusive results can be obtained.

The performance of alloy catalysts can be improved by virtue of the post heat treatments at various temperatures and atmospheres [11,12,19–22]. Moreover, the thermal annealing processes are also extensively applied in the Pt-based alloy catalysts to further enhance their catalytic activity [23,24]. The electro-catalytic activity of Pt–Ru alloy catalysts can be greatly improved due to the alterations in physical structures [25–27], surface compositions [11,12,28], or degrees of Pt–Ru alloying [20,29] after the post heat treatments. Specifically, the post-treatment may induce the change of surface areas and phase separation of Pt and Ru that modify the surface structures along with the intrinsic and mass-specific activities of methanol oxidation [22]. For example, surface Ru atoms exposed in air are easily oxidized. It is also found that pure Ru nanoparticles (NPs) may be fully converted into amorphous RuO_x species after stored in ambient conditions [30,31]. Most likely, the amount of RuO_x species dominated on the surface may exceed that of PtO_x. Therefore, reduction of the Ru oxide layer covered on the outer shell of Pt–Ru alloy particles should result in the Ru-enriched surface of the Pt–Ru alloy catalysts [30]. On the other hand, the study of oxidation treatments induced formation of RuO_x has attracted a great deal of attention. Ru atoms may segregate to the surface of alloy crystallites and are oxidized to crystalline RuO_2 at oxidation temperatures above 520 K [28,32]. The presence of oxidized Ru species in Pt–Ru catalysts results in a promotional electrochemical performance [33]. Moreover, it has also been reported

* Corresponding author. Current address: Institute of Materials Science and Engineering, National Central University, No. 300, Jhongda Rd., Taoyuan 32001, Taiwan. Tel.: +886 3 4227151x34906; fax: +886 3 2805034.
E-mail address: kuanwen.wang@gmail.com (K.-W. Wang).

0925-8388/$ – see front matter © 2010 Elsevier B.V. All rights reserved.
doi:10.1016/j.jallcom.2010.09.096

that the effects of cyclic heat treatment between O_2 and H_2 on the catalytic activity [28]. In the as-received sample, Ru atoms dissolve into the f.c.c. lattice of Pt and produce the well-formed Pt–Ru alloy. However, a non-reversible segregation of RuO_2 from Pt takes place after the treatment [28]. On the contrary, it has been reported that, the Pt–Ru/C catalysts after H_2 treatment at room temperature exhibits the highest activity for MOR due to the mild conditions of the post-treatment. The H_2 and air treatment at 433 K results in the catalysts with lower intrinsic activities due to the phase separation [22].

The heat treatment in N_2 on the catalysts has many advantages, including removal of residual surfactants [20,34] and promotion of the alloying degrees [12,20]. The degrees of alloying of Pt–Ru catalysts depending on the proximity between the Pt and Ru atoms are generally considered as an important structural parameter for MOR efficiency. The alloying effect of Ru atoms into Pt lattice is believed to weaken the adsorption of CO absorbed on the Pt sites due to the modification of the electronic structure [35–37]. However, some researchers still debate on whether the alloyed Pt–Ru or RuO_2 (RuO_xH_y) species is crucial for the enhancement of the MOR activity. Long et al. suggest that the bimetallic alloy is not the most desired form of the catalyst. A mixed-phase electrocatalysts containing Pt metal and hydrous ruthenium oxides (RuO_xH_y) is required to achieve high MOR activity [38]. Ru-decorated Pt catalysts have displayed excellent CO oxidation [39]. Besides, the NPs of Pt deposition on Ru show high activity toward CO and H_2 oxidation [40]. Moreover, Lu et al. show that both increasing the content of hydrous RuO_2 and decreasing the particle size would result in an improved catalytic activity, whereas the effect of the degree of Pt–Ru alloying turn out to be unremarkable [19]. Recently, RuO_2 is used as the support to replace active C in the electrocatalysts [5]. It is found that the RuO_2 ($RuSnO_2$) supported catalysts show an excellent catalytic activity and stability in comparison with Vulcan XC-72 supported catalyst [5], implying RuO_2 may have positive effect on the MOR activity.

Those diverse results may be due to various physical properties of the alloy catalysts, such as alloy structures, surface compositions, and surface species, are not taken into account. Previously, a comparison of surface species from N_2-treated and O_2-treated Pt–Ru alloy catalysts measured by temperature programmed reduction (TPR) has been reported [12]. The results suggest that an alloy with a Pt surface species resulted from N_2 treatment, rather than RuO_2 coming from O_2 treatment, is essential for obtaining a high MOR activity [12].

In this study, a simple procedure of thermal treatment is carried out on the commercial Pt–Ru/C catalysts, which are well known for their long term stability and generally regarded as standard samples in many studies. The alloy catalysts of Pt–Ru/C are purchased from E-TEK Inc. and then subjected to thermal treatments in various environments to modify their electrochemical performance. The MOR activity affected by the alterations of the alloying extents, surface species, and surface segregation has been studied systematically to reveal the SAR of the heat treated catalysts. In terms of surface characterization, X-ray photoelectron spectroscopy (XPS) is applied to estimate the surface composition of NPs with particle size of approximately or large than 3.0 nm [41]. Moreover, TPR can be applied to qualitatively provide the view-point of surface species on the near surface regions of the alloy catalysts [42–48].

2. Experimental

2.1. Modification of catalysts

The carbon black (Cabot Vulcan XC-72R) supported Pt–Ru alloy catalysts were obtained from E-TEK Inc. The catalysts have the nominal loading of 20 wt% and the Pt to Ru atomic ratio was 1 to 1. The as-received catalysts were heated for 1 h at 570 K under flowing air, N_2, or H_2/N_2 (10/90 vol%) at a flow rate of 50 mL/min. The as-received catalysts heated in air, N_2 or H_2/N_2 at 570 K were designated as O570, N570, or H570, respectively. Some H570 and O570 samples were separated into different portions for further heat treatment for 1 h at 570 K under flowing N_2 and were designated as HN and ON, respectively.

2.2. Characterization of catalysts

Physical properties of the as-received and heat-treated catalysts were characterized by X-ray diffraction (XRD). A Guinier powder diffractometer (Huber, Germany), set at 45° transmission angle, was used in this work. A Johansson-type Ge monochromator produced a focused high-intensity monochromatic $CuK_{\alpha 1}$ primary beam ($\lambda = 1.54$ Å) at 40 kV and 20 mA. In the preparation of each sample, a small amount of catalyst (ca. 30 mg) was slightly pressed to a thin pellet of 0.3 mm thickness. This pellet was then fixed between two 3 μm polyethylene foil into the sample holder under ambient conditions. The XRD was operated at a scan rate of 1°/min.

An XPS (Thermo VG Scientific Sigma Probe) using an Al K_α radiation was used to study the surface compositions of the alloy catalysts. The surface compositions of the samples were calculated from the peak areas of the corresponding lines, using a Shirley-type background.

TPR analysis was used to examine the surface species of the heat treated catalysts. In each TPR analysis, a sample of ca. 20 mg was inserted into a tube reactor and pre-oxidized at ambient temperature (300 K) for 1 h. The pre-oxidized catalysts were reduced by a flow of 20% H_2 in N_2 at a flow rate of 30 mL min^{-1} while increasing the temperature from 200 to 500 K at a heating rate of 7 K min^{-1}. Temperature profiles and the hydrogen consumption were measured by a thermal conductivity detector (TCD).

2.3. Electrochemical measurements

Cyclic voltammograms (*CV*): electrochemical measurements (using a CH Instruments Model 600B device) were conducted in a standard three-compartment electrochemical cell with reference and counter electrodes in separate compartments from the working electrode. The preparation of working electrode was described in detail as follows: Typically, 5 mg of the alloy catalysts (including a commercial catalyst of 20 wt% Pt–Ru/C purchased from E-TEK) in 0.5 mL of 2-propanol and 0.5 mL DI water were dispersed in ultrasonic bath for 30 min, obtaining a well-dispersed catalyst ink. Afterwards, a specific amount of 10 μl slurry was spread on the surface of the glassy carbon electrode (area = 0.393 cm^2) and dried at room temperature. After the evaporation of the catalysts ink, the electrode was then transferred to the electrochemical experiments carried out in N_2-saturated electrolyte consisting of 0.5 M H_2SO_4 + 1.0 M methanol. A saturated calomel electrode (SCE) electrode and a Pt plate were served as reference and counter electrode, respectively. The reference electrode was separated from the working electrode compartment by a closed electrolyte bridge in order to avoid chloride contamination. Cyclic potentials were swept between −0.24 and 1.2 V (vs. SCE) in a rate of 20 mVs^{-1} at room temperature. All of the reported CV profiles were recorded in the 16th cycle at 298 K. Furthermore, the potentials in this study all referred to that of the NHE.

CO stripping experiments: the preparation route of working electrode for the CO electro-oxidation measurements was similar to that of the CV tests as described above. In brief, a CO voltammetric stripping experiment was performed as follows: CO was adsorbed onto the electrode surface at −0.14 V (vs. SCE) by bubbling the high purity CO gas through 0.1 M $HClO_4$ for 30 min. The CO adsorption time was found to be sufficient to reach the steady state. After the adsorption process, the N_2–saturated 0.1 M $HClO_4$ was used for the CO stripping study. Two CVs were collected between −0.2 and 0.9 V (vs. SCE) at a scan rate of 50 mVs^{-1}. The first potential sweep was carried out to electro-oxidize the adsorbed CO species and the second one to ensure the complete oxidation of the adsorbed species.

3. Results and discussion

Fig. 1 shows the XRD patterns of the as-received and heat-treated Pt–Ru/C catalysts. For the as-received catalysts, peaks located at 2θ ~40.0°, 46.5°, and 69.5° may represent the (1 1 1), (2 0 0), and (2 2 0) patterns of Pt–Ru alloys, respectively. No monometallic Pt, Ru, or RuO_2 diffractions are observed, indicating the as-received sample forms Pt–Ru alloy structure completely. The samples treated at 570 K in N_2, O_2, and H_2 were named as N570, O570, and H570, respectively. Some O570 and H570 samples further treated at 570 K in N_2 were designated as ON and HN, respectively. For N570, H570, and H–N, the patterns display similar reflections of alloyed f.c.c. crystal structure, with some shifts in the position of each reflection peak. The shifts in 2θ are related to the changes of the lattice constant due to the incorporation or segregation of Ru atoms into or from the f.c.c. alloy phase, respectively. In terms of O_2 treatment, the peaks located at about 35.07 and 54.27° are attributed to the (1 0 1) and (2 1 1) diffractions of

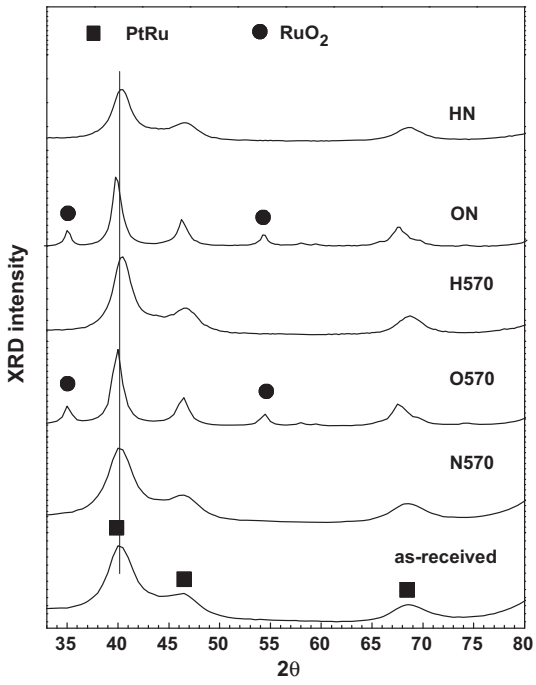

Fig. 1. XRD patterns of the as-received and heat treated Pt–Ru/C catalysts.

RuO_2 (JCPDS 43-1027). The diffraction peaks of RuO_2 are found in all oxidized samples, indicating a portion of Ru atoms segregate out of the alloy phase and aggregate as RuO_2 during the oxidation treatment. Therefore, the Pt core/Ru shell like structure may be observed in the O570 sample, because oxidation of metallic Ru element on its surface is easier than that of the Pt component [49]. The particle size of Pt–Ru alloys (D_{PtRu}) in the as-received sample according to the Scherrer's equation is about 2.0 nm, as listed in Table 1. Heat treatments at 570 K result in the sintering and aggregation of the deposited alloy NPs, especially for the ON sample. The D_{PtRu} of ON and other heat treated samples is about 9.2 and 3.0 nm, respectively.

The third column of Table 1 compares the lattice parameters of various catalysts calculated from (2 2 0) and (2 0 0) reflections shown in Fig. 1. As listed in Table 1, the lattice parameters of the as-received Pt–Ru/C increase through all kinds of heat-treatments, suggesting that the replacement of the Ru atoms in the alloy phase by Pt atoms and the occurrence of the dealloying processes. The lattice constant values for all catalysts should be lower than that of Pt/C (3.9155 Å), and higher than that of Pt–Ru alloy (3.8535 Å) [50]. For the O570 and O–N samples, the lattice parameters are significantly extended, especially for O–N. The lattice parameter of O–N sample is larger than that of Pt/C and close to the metallic one, indicating the Pt–Ru alloy NPs separate from the C support during heat treatment. Furthermore, the Ru atomic fractions, X_{Ru} in the

Table 1
The XRD analysis of the as-received and various heat treated Pt–Ru/C catalysts.

PtRu/C	D_{PtRu} (nm)	Lattice constant (Å)	X_{Ru} (%)	Alloying degree (%)
As-received	2.0	3.855	48.8	97.6
N570	2.6	3.887	23.1	46.1
O570	2.9	3.893	18.6	37.1
H570	3.4	3.875	33.0	66.0
ON	9.2	3.923	–	–
HN	3.4	3.859	45.5	91.0

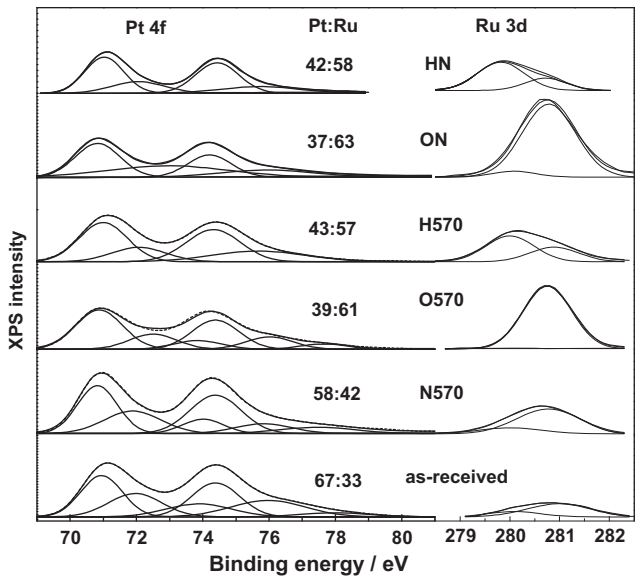

Fig. 2. XPS spectra of the as-received and heat treated Pt–Ru/C catalysts.

Pt–Ru alloys are calculated by the Vegard's law [51,52]:

$$I_{PtRu} = I_{os} - kX_{Ru} \quad (1)$$

where I_{os} = 3.9155 Å is the lattice parameter of pure Pt/C, and k = 0.124 Å is a constant. Table 1 displays the values of X_{Ru} calculated from Eq. (1) and the amount of Ru alloyed (Ru_{al}) calculated from the equation:

$$Ru_{al} = \frac{X_{Ru}}{\left[(1 - X_{Ru})(Ru/Pt)_{nom}\right]} \quad (2)$$

where $(Ru/Pt)_{nom}$ is the nominal Ru/Pt atomic ratio, which is 1 in this study. As shown in Table 1, the as-received sample shows an excellent degree of alloying and the amount of Ru alloyed decreases as the lattice constant increases after various heat treatments. It has been reported that the as-received Pt–Ru/C catalysts are in a single phase state of perfect alloying by in situ XRD measurement [18]. Compared with the values of alloying degrees listed in Table 1, the oxidation treatment results in a significant decrease in the alloying degree, implying that most Ru atoms are oxidized. On the other hand, N_2 and H_2 treatments may cause the structural reconstruction and reduction of RuO_2 of the alloy catalysts, respectively, and the alloying degree of the catalysts also decreases. Moreover, the reduction of RuO_2 during H_2 treatment layer covered on the outer shell results in the Ru-enriched surface [18].

The XPS spectra of the as-received and heat-treated Pt–Ru/C catalysts are exhibited in Fig. 2. The surface compositions of the samples calculated from the peak areas of the corresponding lines in the original spectra (Fig. S1 of supplementary information), using a Shirley-type background is also compared. For the Pt 4f spectra, the deconvolution shows the presence of two or three pairs of doublets. The intense doublet peaks with binding energies of approximately 71.3 (Pt $4f_{7/2}$) and 74.6 eV (Pt $4f_{5/2}$) are attributed to the metallic Pt. The peaks corresponding to about 72.2 and 76.4 eV can be assigned to the Pt(II) species in the form of $Pt(OH)_2$, and the peak located at 74.4 and 77.9 eV can be regarded as PtO_2. On the other hand, the Ru spectra exhibit a distinctive Ru $3d_{5/2}$ peak with the characteristic binding energy for Ru (~280.1 eV) and RuO_2 (281 eV). Apparently, different atmospheres and procedures of heat treatments may result in different compositions and valence states of Pt and Ru species on the catalysts. The surface compositions of various catalysts analyzed by XPS are displayed in Table 2. The

Table 2
Catalytic activities and surface characterizations of the as-received and various heat treated Pt–Ru/C catalysts.

PtRu/C	Surface composition (at%) ($Pt:Pt^{2+}:Ru:Ru^{4+}$)	I_{07} ($A\,cm^{-2}\,mg\,(PtRu)^{-1}$)	I_f/I_b ratio	TPR surface species
As-received	38:29:8:25	0.49	2.1	Pt^sO_x, $A^{Pt}O_x$
N570	36:22:8:34	0.61	1.8	Pt^sO_x, $A^{Pt}O_x$
O570	14:25:1:60	0.20	1.4	Ru^cO_2, Ru^aO_2
H570	32:11:35:22	0.41	2.4	Pt^sO_x, $A^{Pt}O_x$
ON	19:18:59:4	0.43	1.2	Ru^aO_2
HN	30:12:27:31	0.47	2.2	Pt^sO_x, $A^{Pt}O_x$

surface of the as-received Pt–Ru/C catalysts is consisted of mainly RuO_2, Pt, and some $Pt(OH)_2$. Their surface Pt composition is about 67% (38% in metallic state and 29% in oxide state), deviated from the nominal value of 50%. The Pt atoms enriched on the outer surface and Ru atoms partially occupied in the inner core then proceed different degrees of migration and segregation under various atmospheres. It has been reported that the bulk compositions of Pt–Ru/C determined by in-situ extended X-ray absorption fine structure (EXAFS) and XRD. Both techniques show that the surfaces of the particles are enriched with Pt compared to the nominal bulk composition [53]. The in situ XRD measurement suggests that the fraction of surface oxides found is 25 wt% for Pt–Ru/C [30], smaller than the value measured by XPS in this study. In terms of unsupported Pt–Ru catalysts, CV scans in 0.5 M H_2SO_4 solution show hydrous Ru oxide, a proton and electron conductor which favors CO and MOR, is detected as one of the constituent phases in the electrocatalyst and XPS spectra indicate the presence of Pt and Ru in different oxidation states, with larger proportion of the metallic forms [27]. For O570 sample, surface Pt compositions are about 39%, suggesting that 11% extra Ru atoms segregate out from the interior to the surface and form RuO_2 during oxidation treatment. The O_2 treatment causes the significant surface Ru segregation and an obvious decrease in the alloying degree. Finally, O_2 treatment may turn the Pt-rich surface into RuO_2-rich surface (60% on the surface). On the contrary, Pt and Ru oxides are reduced to their metallic states during the H_2 treatment. The reduction of RuO_2 on the H570 sample also enhances the surface Ru segregation and its surface is composed of metallic Pt, Ru, and some RuO_2 (31, 35, and 22%, respectively). It is interesting to find that during the H_2 treatment, the amount of surface RuO_2 does not decrease very much (25–22%), instead, the amount of surface metallic Ru increases significantly from 8% to 35%. Therefore, the oxidation or reduction process of Ru species dominates during the O_2 or H_2 heat treatments, respectively. It is worthy mentioning that according to the thermodynamics, Pt with lower surface energy than that of Ru should have the driving force to segregate out to the alloy surface [54]. Therefore, the Pt surface segregation driven by the surface energy and Ru surface segregation driven by atmospheric attraction competes with each other. As a result, surface segregation of Ru induced by the atmospheric attraction is noted.

On the other hand, for the N570 sample, neither oxidation nor reduction process dominates. Surface Ru segregation takes place to a small extent (from 33% to 42%). The N_2 treatment may serve as an adjustment process for the surface composition and structure of the alloy catalysts which not only changes the surface Pt composition but also slightly oxidizes surface Ru to RuO_2. Even after heating to 920 K in N_2, the Pt–Ru/C catalysts do not show a phase separation, implying N_2 treatment serves as a moderate adjustment process [12,30].

The heat treatments of the catalysts in N_2, O_2, or H_2 not only influence their lattice constants and degrees of Ru alloying on the Pt–Ru/C catalysts but also affect their surface compositions substantially. However, in the case of ON and HN samples (O570 and H570 sample further treated at 570 K in N_2), as shown in Table 2, their surface compositions do not change very much after the 2nd stage of N_2 treatment. The surface Ru composition increases from 61% to 63% and 57% to 58% for the ON and HN, respectively. Only 1–2% of surface Ru segregation occurs in these processes, implying that N_2 treatment serves as the reconstruction and adjustment process during the stage. Only few changes in alloying degrees of the catalysts and valence states of the surface species are observed on the ON and HN samples, as evidenced in Table 1.

Fig. 3 compares the TPR traces of various catalysts. TPR analysis is a surface sensitive technique which can probe surface species of bimetallic Pt–Ru particles deposited on support [11,12,55]. The analytic results from TPR may be not consistent with those from XPS due to their different surface resolutions [40]. The sampling depth of TPR is about several Å (the thickness of the outermost surface layer) and that of XPS is within a few nanometers. Based on the T_r position in TPR traces, the surface species of the alloy catalysts can be analyzed. The surface species of all samples are listed in the final column of Table 2. As shown in Fig. 3, the main reduction peak for the as-received catalysts located between 230 and 250 K is assigned to the reduction of the Pt oxide surface species (Pt^sO_x). The T_r located between 250 and 350 K and above 350 K are attributed to reductions of alloy oxides ($A^{Pt}O_x$ or $A^{Ru}O_x$) and RuO_2, respectively. The $T_r \sim 360$ and 450 K is assigned to the reduction of amorphous (Ru^aO_2) and crystalline (Ru^cO_2) RuO_2, respectively [11]. Therefore, as shown in Fig. 3, the surface of N570 catalysts consists of $A^{Pt}O_x$ mainly, and the surface of O570 is composed of Ru^aO_2 or Ru^cO_2. The N_2 treatment results in a change of the surface species from

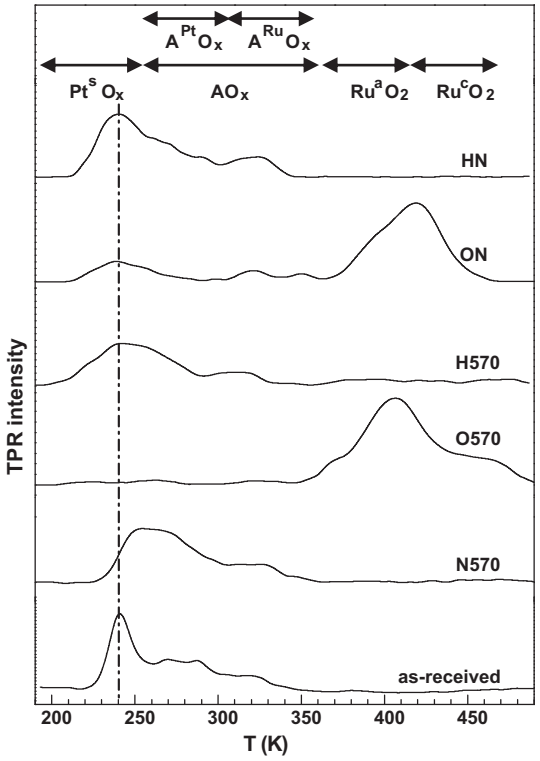

Fig. 3. TPR traces of the as-received and heat treated Pt–Ru/C catalysts.

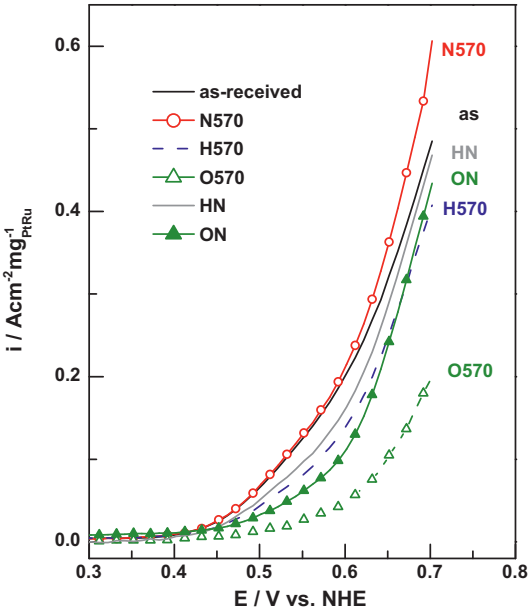

Fig. 4. Forward scans of CV results for the as-received and heat treated Pt–Ru/C catalysts measured at 298 K.

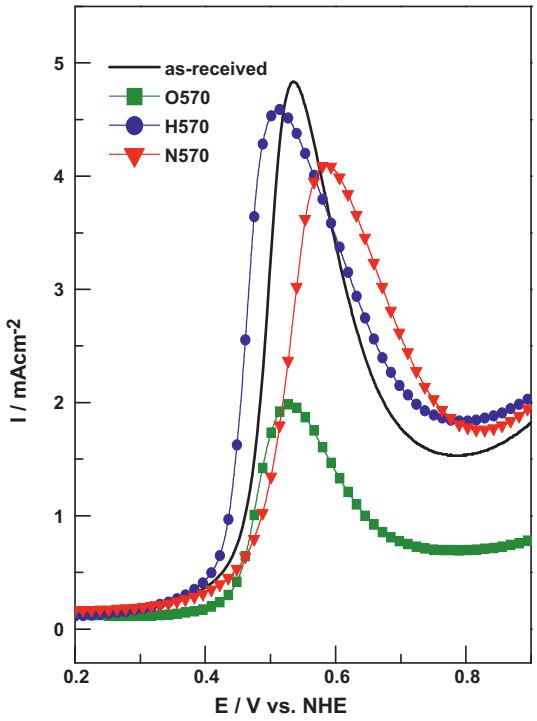

Fig. 5. CO stripping curves for the as-received and various heat treated Pt–Ru/C catalysts.

Pt^sO_x to $A^{Pt}O_x$ while the air treatment causes the oxidation of Ru. On the other hand, H_2 treatment results in a surface composed of both Pt^sO_x and $A^{Pt}O_x$.

Compared with the TPR traces of O570 and ON or H570 and HN samples, it is interesting to find that surface species does not change obviously during the 2nd stage of N_2 treatment. As mentioned above, the surface compositions measured by XPS analyses displayed in Table 2 confirm the result. The N_2 treatment may serve as a moderate treatment process for those samples. Neither surface compositions nor surface species are changed significantly, suggesting that their surface conditions are fixed and only structural properties such as alloying degree or particle sizes are influenced by the treatments slightly.

Fig. 4 displays the forward scans of CV for MOR over the as-received and various heat-treated Pt–Ru/C catalysts at room temperature. The methanol oxidation current at I_{07} (current density at an applied potential of 0.7 V) serves as an indicator for estimating the activity of catalysts under practical conditions. In Fig. 4, the I_{07} of N570 is higher than that of the as-received catalysts, suggesting that N_2 treatment at 570 K is a superior process for the promotion of the MOR for alloy catalysts [12]. On the other hand, the I_{07} of H570 and O570 catalysts are inferior to that of the as-received one. The H_2 and O_2 heat treatments on the Pt–Ru/C catalysts result in some extents of structural and surface changes on the catalysts and therefore inactivate and deteriorate the onset potentials and I_{07} of the catalysts. The O_2 treatment causes the significant surface Ru segregation and an obvious decrease in the alloying degree. The Pt-rich surface of the as-received sample turns into RuO_2-rich surface (60%) after O_2 treatment. As a result, O_2 treatment contributes to the passivation of the Pt–Ru/C catalysts. The I_{07} and I_f/I_b ratio (the ratio of forward to backward peak current density) of various catalysts based on the CV scans are listed in Table 2. Compared to the as-received catalyst, the I_{07} of N570, O570, and H570 is enhanced 24%, decreased 60%, and decreased 16%, respectively. In terms of H570, H_2 treatment also results in significant Ru segregation of the catalysts, however, the catalysts still have high degree of alloying. There are 57% of Ru atoms on the surface and 43% of Ru atoms involved in the alloy phase. As a result, H570 has the extraordinarily high I_f/I_b ratio and H_2 treatment may inhibit the accumulation of CO on Pt sites and thus make the Pt sites free significantly. However, H_2 treatment cannot enhance the anodic current density directly. This excellent CO resistance of H_2-treated catalysts can be related to the high metallic Ru surface composition as well as the high degree of alloying in the H570 sample.

On the other hand, the N570 catalyst containing 58% of surface Pt and $A^{Pt}O_x$ rich surface species displays the highest electrochemical performance toward MOR among all catalysts. This observation is consistent with Wiltshire et al.'s results that in the Pt–Ru alloy with Pt-rich surface, surface fraction of Pt > 0.59 by XPS is the most active [53]. N_2 treatment modifies the surface Pt/Ru ratios from 2.03 to 1.38 and enhances the formation of $A^{Pt}O_x$. The segregated surface Ru atoms are then alloyed with Pt and results in a positive shift in the TPR profile. Moreover, after the 2nd stage of N_2 treatment, the observed I_{07} and onset potential in HN and ON samples is both enhanced. N_2 treatment results in a roughly 200% enhancement on the I_{07} of O570 where I_{07} of O570 and ON is 0.20 and 0.43 A cm^{-2} mg $(PtRu)^{-1}$, respectively. The enhancement is owing to the changes in the alloying degrees and valence states of Pt and Ru.

According to the electrochemical performance and the physical measurements of various catalysts, we can find that the degree of alloying may not play a paramount role in the enhancement of MOR activity. Instead, the surface compositions and surface species may be considered as important parameters to obtain high catalytic activity. Although the poor alloying extent is observed in N_2-treated sample, the surface mainly comprised of $A^{Pt}O_x$ species presents the best performance toward MOR among all samples. Therefore, N_2 treatment process instead of O_2 or H_2 treatment on the Pt–Ru alloy catalysts is the best way to promote the MOR activity. H_2 treatment can enhance the de-poisoning ability of the catalyst, as evidenced by the high I_f/I_b values of H570 and HN samples. On the other hand, the formation of RuO_2 has negative effect both in the MOR activity and CO resistance.

Fig. 5 shows the CO stripping scans recorded on the glassy carbon electrode of various PtRu/C catalysts in 0.1 M $HClO_4$. It is generally accepted the fact that the activity for electrochemically

Table 3
Comparative CO oxidation results of the as-received and various heat treated Pt–Ru/C catalysts.

Sample	E_{onset} (V)	E_{peak} (V)	EASA (m^2/g_{Pt})
As-received	0.46	0.58	158.7
N570	0.46	0.63	156.3
O570	0.46	0.57	68.0
H570	0.42	0.55	194.1

oxidizing adsorbed CO on the catalysts and the real electrochemical active surface area (EASA) of the catalysts can be probed by CO stripping technique [54–57]. The clearly difference in EASA for as-received and heat-treated samples is found and provided in Table 3. Obviously, it should be noted that the high EASA value of H570 may be attributed to the appearance of metallic Pt, Ru or PtO_x species on the surface of the catalysts as evidenced by XPS and TPR results. This phenomenon is in agreement with the experimental results stated by Hwang et al. that the enhanced CO oxidation current density of H_2-treated catalysts is owing to the increased population of Pt on the surface revealed by XAS results [58]. For the O570 sample, the dramatically decreased EASA is observed due to a large amount of RuO_2 species occupied on the surface and a decrease in the number of Pt active sites accordingly. On the contrary, it can be unambiguously perceived that the H570 displays the lower onset potential for CO electro-oxidation compared to that of the others, indicating that numerous metallic Ru on the surface (ca. 66%) may assist the CO oxidation through a bifunctional mechanism [53]. Herein, we can summarize that the H570 has high I_f/I_b value, high EASA, and low onset potential for anodic CO stripping is probably assigned to the metallic Pt and Ru or PtO_x species on the surface [42,58]. Nevertheless, the H570 cannot exhibit a comparative catalytic activity toward methanol decomposition at I_{07}, suggesting that the surface amount of active sites for MOR is not sufficient. Instead, the N570 produces approximately 24% improvement of MOR performance, implying that the alloy catalysts surface mainly comprised of the $A^{Pt}O_x$ and 60% surface Pt species plays a crucial role in presenting extraordinary catalytic performance.

4. Conclusions

The importance of degrees of Pt–Ru alloying, surface Ru oxide species, and surface compositions of the Pt–Ru/C catalysts toward the MOR activity has been elucidated. A commercial Pt–Ru/C alloy catalysts have been heat treated in various atmospheres to investigate their SAR. The physical properties of various alloy catalysts have been characterized by CV, XRD, XPS, and TPR. The as-received Pt–Ru/C catalysts have a Ru rich in the inner core and Pt rich on the outer shell structure. O_2 treatment results in obvious Ru segregation and formation of RuO_2, which does not benefit to the MOR electro-activity and CO resistance. Reduction of RuO_2 of catalysts during H_2 treatment also causes metallic Ru segregation with the retained alloy degree. These may be the reasons that catalysts treated by H_2 have high I_f/I_b values in the CV scans and an excellent CO de-poisoning ability during the CO stripping measurement. N_2 treatment may serve as an adjustment process for surface composition and structure of the alloy catalysts. For the N570 sample, the surface Pt composition is about 60% and $A^{Pt}O_x$ is the dominant surface species, thus the MOR is enhanced. For the HN and ON samples, their Pt/Ru ratios and surface species are fixed. The enhancement of MOR is attributed to the adjustment of the alloying degrees and surface valence states of Pt and Ru by N_2 treatment. N_2 treatment instead of O_2 or H_2 treatment is the best way to promote the MOR activity.

Acknowledgement

This work was supported by the National Science Council of Taiwan under Contract No. NSC-99-2221-E-008-058.

Appendix A. Supplementary data

Supplementary data associated with this article can be found, in the online version, at doi:10.1016/j.jallcom.2010.09.096.

References

[1] A. Hamnett, Catal. Today 38 (1997) 445.
[2] X. Ren, M.S. Wilson, S. Gottesfeld, J. Electrochem. Soc. 143 (1996) L12.
[3] T.R. Ralph, M.P. Hogarth, Platinum Met. Rev. 46 (2002) 146.
[4] M.S. Kim, B. Fang, N.K. Chaudhari, M. Song, T.S. Bae, J.S. Yu, Electrochim. Acta 55 (2010) 4543.
[5] J.M. Lee, S.B. Han, Y.W. Lee, Y.J. Song, J.Y. Kim, K.W. Park, J. Alloy Compd. 506 (2010) 57.
[6] M. Watanabe, S. Motoo, J. Electroanal. Chem. 60 (1975) 267.
[7] O.A. Petrii, J. Solid State Electrochem. 12 (2008) 609.
[8] W. Vielstich, A. Lamm, H.J. Gasteiger, Handbook of Fuel Cell Technology, Wiley, New York, 2003.
[9] H.B. Yu, J.H. Kim, H.I. Lee, M.A. Scibioh, J. Lee, J. Han, S.P. Yoon, H.Y. Ha, J. Power Sources 140 (2005) 59.
[10] A.M. Zainoodin, S.K. Kamarudin, W.R.W. Daud, Int. J. Hydrogen Energy 35 (2010) 4606.
[11] K.W. Wang, S.Y. Huang, C.T. Yeh, J. Phys. Chem. C 111 (2007) 5096.
[12] Y.C. Wei, C.W. Liu, K.W. Wang, ChemPhysChem 10 (2009) 1230.
[13] Z.G. Shao, F. Zhu, W.F. Lin, P.A. Christensena, H. Zhang, Phys. Chem. Chem. Phys. 8 (2006) 2720.
[14] K. Matsuok, K. Miyazaki, Y. Iriyama, K. Kikuchi, T. Abe, Z. Ogumi, J. Phys. Chem. C 111 (2007) 3171.
[15] Z.B. Wang, P.J. Zuo, G.P. Yin, J. Alloy Compd. 479 (2009) 395.
[16] Y. Liang, J. Li, Q.C. Xu, R.Z. Hu, J.D. Lin, D.W. Liao, J. Alloy Compd. 465 (2008) 296.
[17] J.M. Sieben, M.M.E. Duarte1, C.E. Mayer, J. Alloy Compd. 491 (2010) 722.
[18] D.J. Guo, J. Power Sources 195 (2010) 7234.
[19] Q. Lu, B. Yang, L. Zhuang, J. Lu, J. Phys. Chem. B 109 (2005) 8873.
[20] X. Li, I.M. Hsing, Electrochim. Acta 52 (2006) 1358.
[21] D.B. Kim, H.J. Chun, Y.K. Lee, H.H. Kwon, H.I. Lee, Int. J. Hydrogen Energy 35 (2010) 313.
[22] K.S. Lee, H.Y. Park, Y.H. Cho, I.S. Park, S.J. Yoo, Y.E. Sung, J. Power Sources 195 (2010) 1031.
[23] K.J.J. Mayrhofer, V. Juhart, K. Hartl, M. Hanzlik, M. Arenz, Angew. Chem. Int. Ed. 48 (2009) 3529.
[24] T.Y. Jeon, S.J. Yoo, Y.H. Cho, K.S. Lee, S.H. Kang, Y.E. Sung, J. Phys. Chem. C 113 (2009) 19732.
[25] D.G. Liu, J.F. Lee, M.T. Tang, J. Mol. Catal. A 240 (2005) 197.
[26] B.J. Hwang, L.S. Sarma, J.M. Chen, C.H. Chen, S.C. Shih, G.R. Wang, D.G. Liu, J.F. Lee, M.T. Tang, J. Am. Chem. Soc. 127 (2005) 11140.
[27] A. Velazquez-Palenzuela, F. Centellas, J.A. Garrido, C. Arias, R.M. Rodrıguez, E. Brillas, P.L. Cabot, J. Phys. Chem. C 114 (2010) 4399.
[28] S.Y. Huang, C.M. Chang, K.W. Wang, C.T. Yeh, ChemPhysChem 8 (2007) 1774.
[29] B.J. Hwang, C.H. Chen, L.S. Sarma, J.M. Chen, G.R. Wang, M.T. Tang, D.G. Liu, J.F. Lee, J. Phys. Chem. B 110 (2006) 6475.
[30] W. Vogel, J. Phys. Chem. C 112 (2008) 13475.
[31] W. Vogel, V. Le Rhun, E. Garnier, N. Alonso-Vante, J. Phys. Chem. B 105 (2001) 5238.
[32] S.Y. Huang, S.M. Chang, C.L. Lin, C.H. Chen, C.T. Yeh, J. Phys. Chem. B 110 (2006) 23300.
[33] E.S. Steigerwalt, G.A. Deluga, D.E. Cliffel, C.M. Lukehart, J. Phys. Chem. B 105 (2001) 8097.
[34] Z. Liu, X.Y. Ling, X. Su, J.Y. Lee, J. Phys. Chem. B 108 (2004) 8234.
[35] P. Waszczuk, A. Wieckowski, P. Zelenay, S. Gottesfeld, C. Coutanceau, J.M. Leger, C.J. Lamy, Electroanal. Chem. 511 (2001) 55.
[36] C. Roth, N. Benker, T. Buhrmester, M. Mazurek, M. Loster, H. Fuess, D.C. Koningsberger, D.E. Ramaker, J. Am. Chem. Soc. 127 (2005) 14607.
[37] C. Lu, C. Rice, M.I. Masel, P.K. Babu, P. Waszczuk, H.S. Kim, E. Oldfield, A. Wieckowski, J. Phys. Chem. B 106 (2002) 9581.
[38] J.W. Long, R.W. Stroud, K.E. Swider-Lyons, D.R. Rolison, J. Phys. Chem. B 104 (2000) 9772.
[39] F. Maillard, G.Q. Lu, A. Wieckowski, U. Stimming, J. Phys. Chem. B 109 (2005) 16230.
[40] J.X. Wang, S.R. Brankovic, Y. Zhu, J.C. Hanson, R.R. Adzic, J. Electrochem. Soc. 150 (2003) A1108.
[41] D. Briggs, M.P. Seah, Practical Surface Analysis, vol. 1, Wiley, New York, 1990.
[42] S.Y. Huang, S.M. Chang, C.T. Yeh, J. Phys. Chem. B 110 (2006) 234.
[43] C.W. Liu, Y.C. Wei, K.W. Wang, Electrochem. Commun. 11 (2009) 1362.
[44] C.W. Chou, S.J. Chu, H.J. Chiang, C.Y. Huang, C.J. Lee, S.R. Sheen, T.P. Perng, C.T. Yeh, J. Phys. Chem. B 105 (2001) 9113.

[45] K.W. Wang, S.R. Chung, C.W. Liu, J. Phys. Chem. C 112 (2008) 10242.
[46] C.W. Liu, Y.C. Wei, K.W. Wang, J. Colloid Interface Sci. 336 (2009) 654.
[47] Y.W. Chang, C.W. Liu, Y.C. Wei, K.W. Wang, Electrochem. Commun. 11 (2009) 2161.
[48] Y.C. Wei, C.W. Liu, Y.W. Chang, C.M. Lai, P.Y. Lim, L.D. Tsai, K.W. Wang, Int. J. Hydrogen Energy 35 (2010) 1864.
[49] N.Y. Hsu, C.C. Chien, K.T. Jeng, Appl. Catal. B: Environ. 84 (2008) 196.
[50] E. Antolini, F. Cardellini, L. Giorgi, J. Mater. Sci. Lett. 19 (2000) 2099.
[51] D. Chu, S. Gilman, J. Electrochem. Soc. 143 (1996) 1685.
[52] H.A. Gasteiger, P.N. Ross, E.J. Cairns, Surf. Sci. 293 (1993) 67.
[53] R.J.K. Wiltshire, C.R. King, A. Rose, P.P. Wells, H. Davies, M.P. Hogarth, D. Thompsett, B. Theobald, F.W. Mosselmans, M. Roberts, A.E. Russell, Phys. Chem. Chem. Phys. 11 (2009) 2305.
[54] A. Cuesta, A. Couto, A. Rincon, M.C. Perez, A.L. Cudero, C. Gutierrez, J. Electroanal. Chem. 586 (2006) 184.
[55] A. Pozio, M.D. Francesco, A. Cemmi, L. Giorgi, J. Power Sources 105 (2002) 13.
[56] T. Vidaković, M. Christov, K. Sundmacher, Electrochim. Acta 52 (2007) 5606.
[57] L. Vitos, A.V. Ruban, H.L. Skriver, J. Kollar, Surf. Sci. 411 (1998) 186.
[58] B.J. Hwang, L.S. Sarma, G.R. Wang, C.H. Chen, D.G. Liu, H.S. Sheu, J.F. Lee, Chem. Eur. J. 13 (2007) 6255.